Published OnlineFirst April 19, 2019; DOI: 10.1158/1078-0432.CCR-18-3261

Translational Cancer Mechanisms and Therapy

Clinical Cancer Research

A Constitutional Activating *MET* Mutation Makes the Genetic Link between Malignancies and Chronic Inflammatory Diseases

Morad El Bouchtaoui[1], Marcio Do Cruzeiro[2], Christophe Leboeuf[1,3], Irmine Loisel-Ferreira[1,3], Carèle Fedronie[4], Chrystophe Ferreira[5], Rachida Ait El Far[1], Marianne Ziol[6,7,8], Marc Espié[9], Géraldine Falgarone[10], Bruno Cassinat[11], Jean-Jacques Kiladjian[12], Jean-Paul Feugeas[13,14], Anne Janin[1,3,15], and Guilhem Bousquet[1,3,10,16]

Abstract

Purpose: The genesis of all cancers results from an accumulation of mutations, constitutional and/or acquired when induced by external mutagenic factors. High-speed technologies for genome sequencing have completely changed the study of disease genetics, but with limited knowledge of the functional value of most genetic changes.

Experimental Design: Here, we proposed an innovative individual approach by studying tissue samples from a young woman with an unusual association of breast cancer, polycythemia vera, and rheumatoid arthritis. We performed genomic analyses for copy number variations and point mutations on laser-microdissected tumor cells from the breast cancer, and on $CD34^+$ cells sorted from bone marrow aspiration, to identify gene abnormalities common to these two types of cell populations.

Results: Using ONCOSCAN technology, we identified a constitutional pR988C, c2962C>T mutation of *MET*. Using CRISPR-Cas9 technology, we established pR988C *MET*-mutated transgenic mice, which reproduced the autoimmune diseases and myeloproliferation found in our index-case; one of the transgenic mice spontaneously developed a skin squamous cell carcinoma. We also showed that additional mutagenic factors were required to induce cancers, including skin squamous cell carcinoma and thyroid cancer. Using an anti-MET drug, cabozantinib, we demonstrated for the first time the functional role of this mutation in the maintenance of myeloproliferation and rheumatoid arthritis, and in cancer genesis.

Conclusions: Our study opens a considerable field of application in the domain of constitutional genetics, to establish genetic links between cancers and other very different severe diseases.

Introduction

New high-speed technologies for genome sequencing have completely changed the study of cancer genetics, including constitutional genetics. However, they are usually restricted to identifying mutations in genes of high penetrance responsible for well-known hereditary syndromes (1). On the other hand, most genetic changes detected in whole-genome analyses are of unknown functional value. This is particularly true for genes of low to moderate penetrance.

Five percent to 10% of human cancers are considered to be linked to a constitutional genetic abnormality. Mutations in genes of high penetrance are usually identified using linkage analysis in

[1]INSERM, U1165-Paris, France. [2]Institut Cochin, INSERM U1016, Plateforme de Recombinaison Homologue, Paris, France. [3]Université Paris Diderot, Inserm, UMR-S 1165, Paris, France. [4]INSERM, U944, Paris, France. [5]Université Paris Descartes, Plateforme ANIMA5, Paris, France. [6]Hôpital Jean Verdier, APHP, Service d'Anatomie pathologique, Bondy, France. [7]Université Paris 13, Villetaneuse, France. [8]Université Paris Descartes, Université Paris Diderot, Inserm, UMR_S1162, Génomique Fonctionnelle des Tumeurs Solides, Paris, France. [9]Hôpital Saint-Louis, APHP, Centre des Maladies du Sein, Paris, France. [10]Université Paris 13, Villetaneuse, France. [11]Hôpital Saint-Louis, APHP, Laboratoire de Biologie Cellulaire, Paris, France. [12]Hôpital Saint-Louis, APHP, Centre d'Investigation Clinique, Paris, France. [13]INSERM, U1137-Paris, France. [14]Université de Franche-Comté, Département de Biologie, Besançon, France. [15]Hôpital Saint-Louis, APHP, Service de Pathologie, Paris, France. [16]Hôpital Avicenne, APHP, Service d'Oncologie médicale, Bobigny, France.

Note: Supplementary data for this article are available at Clinical Cancer Research Online (http://clincancerres.aacrjournals.org/).

C. Leboeuf and I. Loisel-Ferreira contributed equally to this article.

A. Janin and G. Bousquet are co-senior authors of this article.

Corresponding Authors: Morad El Bouchtaoui, Inserm U1165, 1 Avenue Claude Vellefaux, Paris 75010, France. Phone: 014-249-4570; Guilhem Bousquet, U1165, 1 avenue Vellefaux, Paris, F-75010, France. Phone: 331-4238-5428; Fax: 331-4249-4922; E-mail: guilhem.bousquet@aphp.fr; and Anne Janin, U1165, Université Paris7, Inserm, Hôpital Saint-Louis. Phone: 331-4249-4570; Fax: 331-4249-9281; E-mail: anne.janin1165@gmail.com

Clin Cancer Res 2019;25:4504–15

doi: 10.1158/1078-0432.CCR-18-3261

Published OnlineFirst April 19, 2019; DOI: 10.1158/1078-0432.CCR-18-3261

Translational Relevance

This study did the proof-of-concept of an innovative individual approach to address constitutional genetics of low penetrance. Our study opens a considerable field of application in the domain of constitutional genetics to establish genetic links between cancers and other very different severe diseases.

families. For genes of lower penetrance, identifying mutations is more difficult. It is based on their cellular functions in families with cancer predisposition (2).

In the case of breast cancer, mutations in genes of high penetrance, including *BRCA1* or *BRCA2*, are now identified in 30% of familial cancer cases (3). Genes of moderate penetrance implicated in DNA repair (*CHEK2*, *BRIP1*, *PALB2*, and *ATM*) have been characterized more recently, and genes of low penetrance are rarely identified because they require systematic studies of large populations with a low risk of cancer and possible polygenic involvement (4). Genome-wide association studies remain the predominant investigation to identify breast cancer susceptibility alleles, and potential new candidate genes (5). A recent meta-analysis of 1,059 publications found a moderate to strong association with breast cancer risk for 14 variants in 9 genes (6). However, the functional value of these 14 variants has not been demonstrated.

Next-generation sequencing applied to cancer has opened the field for individual approaches, through identification of new sporadic genomic abnormalities. Some of them, such as sporadic *BAP1* mutations, have secondarily been considered as potential germline mutations in familial forms of renal cancer (7, 8), although their functional value has not so far been demonstrated.

Here, we propose an innovative individual approach by studying tissue samples from a young woman with an unusual association of cancer and other severe diseases, to identify constitutional mutations of low to moderate penetrance and demonstrate their functional value.

Materials and Methods

DNA purification and whole-genome analysis on human samples

Whole-genome analysis was performed on breast cancer tumor cells, and on $CD34^+$ cells sorted from bone marrow aspiration. In compliance with French bioethics law, the patient had been informed of the research use of the part of her samples remaining after diagnosis had been established, and did not oppose it. Informed consent was obtained according to French bioethics law (2004-800, 06/08/2004). Laser-microdissection (Palm) was used to select breast cancer tumor cells from paraffin-embedded tissue sections. $CD34^+$ cells were obtained through magnetic sorting using anti-CD34 beads antibody (Miltenyi Biotec). DNA was purified using QIAmp DNA Mini Kit (Qiagen), quantified on Nanodrop, and qualified by electrophoresis.

Whole-genome analysis was performed using OncoScan-Express (Affymetrix), a molecular inversion probe (MIP)–based genotyping system that determines the genotype of 330,000 SNPs, copy number alterations, loss of heterozygosity (LOH) and somatic mutations on formol-fixed paraffin-embedded samples. MIP probes are circularizable oligonucleotides, the two ends of which carry two sequences complementary to two sequences on the genome separated by one nucleotide (where the variant to be genotyped is located). After hybridization of the genomic DNA, the reaction product is divided between two tubes, and two nucleotides are added to each tube (A/T and C/G). In the tube including the nucleotide complementary to the allele on the genome, the MIP probe is ligated and becomes circular. This structure is selected using exonucleases, and linearized. The products are amplified and hybridized onto an Affymetrix microarray for product identification (Supplementary Fig. S1). Oncoscan assay searches for 541 somatic mutations specific to cancer, with a coverage of over 200 tumor suppressors and oncogenes, and a median spacing of 1 probe per 0.5 kb for the top 10 "actionable" tumor suppressor genes, a median spacing of 1 probe per 2 kb for the top 190-plus actionable oncogenes, and a median backbone spacing of 1probe per 9 kb.

Here, data analyses for mutation detection were performed on a Nexus-7 software (BioDiscovery).

Detection of the pR988C *MET* mutation

MET mutation was detected using three different methods: PCR high-resolution melting (PCR-HRM), Sanger sequencing, and restriction enzyme digestion.

PCR-HRM analyses of *MET* mutation in human samples (with forward primer 5′-GCCTATCCAAATGAGGAGTGTGT-3′ and reverse primer 5′-TCTGTTTTAAGATCTGGGCAGTGA-3′) were carried out on the the CFX96 Real Time System (Bio-Rad) on a total volume of 20 μL containing 5 μL of genomic DNA (20 ng), 15 μL of SsoFast EvaGreen Supermix 1× (Bio Rad), and 0.4 μmol/L of both forward and reverse primers. The PCR was performed with an initial denaturing step at 94°C for 2 minutes, followed by 45 cycles of denaturation (95°C for 5 seconds) and annealing (60°C for 10 seconds). After PCR, a postamplification melting curve program was initiated by heating to 95°C for 1 minute, cooling to 50°C for 1 minute, and continuously increasing the temperature by 0.2°C to finally reach 95°C. Each PCR run included a no-template control, and each sample was run in triplicate. Postamplification fluorescent melting curves were analyzed with the Bio-Rad Precision Melt Analysis software (Bio-Rad).

Sequencing of the shift fragment determined by PCR-HRM was performed using the Sanger method. Twenty microliters of PCR products were purified using affinity columns (Qiagen). Labeling was performed using BigDye-Terminator-v1.1-Sequencing-Kit (Applied Biosystems) in both forward and reverse directions. The reaction was run with an initial denaturing step at 94°C for 3 minutes, 25 cycles at 94°C for 10 seconds, and annealing temperature at 60°C for 20 seconds. BDX-terminator purified products were run on a 16-capillary automated sequencer (ABI-PRISM-3130xl-GeneticAnalyzer, Applied Biosystems). SeqScape-Software v 2.5 (Applied Biosystems) enabled nucleotide change determination.

For restriction enzyme digestion, about 10 to 15 μL of the amplified PCR product was digested with five units of *Xmn1* restriction enzyme (Promega), and electrophoresis was performed on a 2% agarose gel (Invitrogen).

Published OnlineFirst April 19, 2019; DOI: 10.1158/1078-0432.CCR-18-3261

VHL microsatellite analyses

For microsatellite analyses, allelotyping of a physical distance of approximately 6.5 Mb between markers D3S1597 and D3S3611 was performed using 2 polymorphic microsatellite markers flanking VHL gene and listed in the UCSC database. The primer sequences used for PCR analyses are:

Marker	Location	Sequence of primers
D3S1597	3p25·3	Upstream 5′AGTACAAATACACACAAATGTCTC3′ Downstream 5′GTTTCTTGCAAATCGTTCATTGCT3′
D3S3611	3p25·3	Upstream 5′GCTACCTCTGCTGAGCAT3′ Downstream 5′GTTTCTTTAGCAAGACTGTTGGGG3′

One primer of each microsatellite marker was end-labeled with one of the following fluorophores: HEX or CyS5 (Applied Biosystems). PCR was conducted as follows: for each microsatellite marker, equal amounts of DNA (20 ng each of constitutional and tumor-extracted) were subjected simultaneously in 2 different PCR tubes to one cycle of soaking at 95°C in a CFX96 Real Time System (Bio-Rad), then to 40 cycles of amplification at 95°C for 30 seconds and 60°C for 1 minute. The amplification was terminated by a final extension step at 72°C for 10 minutes. The resulting PCR products were analyzed on an Applied Biosystems 3130xl genetic analyzer using the GeneMapper software. This technique allowed the estimation of allele size and the quantitative evaluation of allele ratio. Homozygous markers were quoted "not informative". Informative cases were scored as LOH when the intensity of the signal for one allele in tumor tissue specimens was decreased by >50% in comparison with allelic signal observed in normal tissue specimens. Allelic imbalance was scored when the signal for one allele was decreased >20% and <50%.

Generation of knock-in transgenic mice for human pR988C *MET* mutation

C57BL/6 mice were purchased from Charles River Laboratories at 3 to 4 weeks of age (Charles River Laboratories). All experiments were performed in accordance with NIH guidelines, and the European Union recommendations (2010/63/UE). The University Institute Board Ethics Committee for experimental animal studies approved this study (N°2012-15/728-0115).

Because the pR988C,c2962C>T *MET* mutation is located on a codon identical in human and mouse genes, we decided to establish knock-in transgenic mice to decipher the function of this point mutation.

MET human sequence at the locus of interest:

3′TCTTTAACAAGCTCTCTCTTTCTCTCTGTTTTAAGATCTGG-GCAGTGAATTAGTTCGCTATGACGCAAGAGTACACACTCCTC-ATTTGGATAGGCTTGTAAGTGCCCGAAGTGTAAGTCCAACTA-CAGAGATGGTTTCAAATGAGT5′

MET mouse sequence at the same locus of interest:

3′TCTTTAACAAGCTCTTTCTTTCTCTCTGTTTTAAGATCTGG-GCAGTGAATTAGTTCGCTA**C**GA**T**GCAAGAGTA**GCAGAAATTG-TTCGA**GAAAG**AAAGAGAGACAAAATTCTAGACCCGT**CA**CT**TA-ATCAAACGATGCTAGCTTCTC**5′

c2962C_T *MET* mutation is highlighted in yellow, and differences between human and mouse are in bold.

The design of CRISPR/Cas9 plasmid was performed using two sgRNAs (http://crispr.mit.edu/, sgRNA 5 and sgRNA 8).

	sequences (5′-3′)
Fwsg5RNA	5′AGGGGAAGAGTACACACTCCTCATT3′
Rvsg5RNA	5′AAACAATGAGGAGTGTGTACTCTTC 3′
Fwsg8RNA	5′AGGGGGTTAAAGACTTTGCTGTCAC 3′
Rvsg8RNA	5′AAACGTGACAGCAAAGTCTTTAACC 3′
ssODN	5′CTGTGACAGCAAAGTCTTTAACAAGCTCTCTCTTT-CTCTCTGTTTTAAGATCTGGGCAGTGAATTAGTT-tGCTATGACGCAAGAGTACACACTCCTCATTTGGA-TAGGCTTGTAAGTGCCCGAAGTGTAAGTCCAACT3′

The sgRNA-Cas9 coexpression plasmid (CMV-T7-hspCas9-T2A-GFP-H1-gRNA linearized SmartNuclease vector) was obtained using the Precision Cas9 SmartNuclease System from SBI (System Bioscience). The plasmid was transfected into *E.Coli* using the One-Shot TOP10 Chemically Competent E. Coli Kit (Invitrogen). After kanamycin selection of transfected bacteria, plasmid DNA was extracted using the PureLink HiPure Plasmid Midiprep Kit (Invitrogen). Female C57BL/6J mice were injected with pregnant mare serum gonadotropin (PMSG) and human chorionic gonadotropin (hCG) with a 48-hour interval, and mated with male C57BL/6J mice. Cas9 mRNA (2 ng/μL) and sgRNAs (5 ng/μL for each sgRNA) targeting sgRNA5 or sgRNA8 were mixed and injected into the pronuclei of the one-cell embryos. After transfection, the zygotes were cultured in M16 Medium at 37°C, until blastocyst stage (around 100 cells) and transferred into pseudopregnant mice. This step was performed in the animal facilities of the Cochin Institute (MDC, CF). When founders were identified, they were transferred to the animal facility of the university institute of hematology for breeding. For each generation, a genotyping was performed on 3-week-old mice.

Genotype of the pR988C *MET* transgenic mice

PCR-HRM and Sanger sequencing were performed for mouse genotyping as described above, using forward primer 5′-GTTTTGTTATTATCCGGGCTCTTCCTGT-3′ and reverse primer 5′-GATATTTCTCAGGATAGTAAACTGAATT-3′.

Restriction enzyme digestion was performed using *XmnI* enzyme as described above.

The number of off-targets was assessed using copy number variation.

Droplet Digital PCR (ddPCR) was performed using the QX100 ddPCR workflow system (Bio-Rad) to analyze copy number variation (CNV). The mix contained 20 ng of genomic DNA, 10 μL of ddPCR Supermix for probes (no dUTP; Bio-Rad), 1 μL of *MET* probes (Mm00192978_cn, Life Technologies), and 1 μL *TFrc* probes (TaqMan copy number Reference Assay, 4458366, Life Technologies) per well, with a final mix volume of 20 μL. The PCR mix was then poured into the middle wells of DG8 cartridges for the QX100 Droplet Generator (Bio-Rad), and 70 μL of droplet generation oil (Bio-Rad) was added to the bottom wells of the same cartridges. After sealing, the cartridges were placed in the Bio-Rad QX200 Droplet Generator System (Bio-Rad). The final volume of droplets in oil was approximately 40 μL. PCR was carried out on the CFX96 Real Time System (Bio-Rad), with an initial denaturing step at 95°C for 10 minutes, followed by 40 cycles of denaturation (95°C for 15 seconds), and annealing (60°C for 1 minute). A postamplification melting curve program was initiated by heating to 98°C for 10 minutes and then cooling down to 12°C. Each PCR run included a no-template control. The results of ddPCR were generated using QX100 Droplet Reader

Published OnlineFirst April 19, 2019; DOI: 10.1158/1078-0432.CCR-18-3261

(Bio-Rad), and analyzed using QuantaSoft software (Bio-Rad). The ratio of pR988C *MET*-positive droplets to *TFrc*-positive droplets was calculated.

Phenotype of pR988C *MET* transgenic mice

Blood and bone marrow analyses were performed at three different time points for each mouse. At euthanasia, all organs, including bone marrow, were systematically dissected for further tissue analyses. All tissue samples were similarly processed and cut into two parts: one was formaldehyde-fixed and paraffin-embedded, one was snap-frozen in liquid nitrogen and stored in Hôpital-Saint-Louis Tumorbank. All tissue sections were performed with HM-340 automatic microtome (Microm) at 5 μm and stained with hematoxylin–eosin (H&E). Two pathologists (A. Janin, G. Bousquet) performed the tissue analyses.

For auto-immunity assessment, the level of auto-antibodies in each mouse serum was measured using ELISA for anti-SSA, anti-SSB, anti-dsDNA, anti-CENT (Sygnosis), and anti-CCP (Interchim) according to the manufacturers' protocols.

Blood cell counts were obtained using MS9-5 Hematology Analyzer (Melet Schloesing).

For bone marrow analysis, cells aspirated from femurs of each mouse were suspended in PBS/SVF 2%. Red Blood Cells Lysis Buffer (Sigma Aldrich) was used before staining. Hematopoietic stem cell (HSC), multipotent hematopoietic progenitors (MPP), myeloid progenitors (MP), granulocyte monocyte precursor (PreGM), granulocyte-monocyte progenitor (GMP), megakaryocyte erythroid progenitor (MEP), Erythroid progenitor (EryP), and megakaryocyte progenitor (MkP) populations were stained with a panel of rat anti-mouse antibodies (all Sony Biotechnologies) including the PacBlue lineage cocktail (B220, Ter-119, CD3e, Gr-1, CD11b), PercpCy5.5 CD117 (Clone 2B8), PE/Cy7 Sca-1(Clone D7), BUV737 CD16/32 (Clone 2.4G2), Brilliant Violet 650 CD150 (Clone TC15-12F12.2), Alexa Fluor 647 CD105 (Clone MJ7/18), Brilliant Violet 605 CD41 (Clone MWReg30). The XMP population appears as an undefined myeloid progenitor. All experiments were performed using a FACs LSR Fortessa (BD Biosciences) according to the gating strategy shown in Extended Data (Behrens and al., 2016) and analyzed with FlowJo software (FlowJo, LLC).

Functional inhibition of the *MET* pathway

The mice were treated with cabozantinib (Sellekchem), a MET inhibitor in the tyrosine kinase domain, at the dose of 30 mg/kg, by daily gavage over one month. The drug was diluted in 100 mL of NaCl with 2% of DMSO.

To assess treatment efficacy, we performed bone marrow aspirations and blood analyses at three time points: before treatment, after one month of treatment, and after a wash-out period of 2 weeks following the end of treatment.

Auto-immunity and bone marrow analyses were performed as described above.

Tumor induction experiments

Remaining MET-mutated transgenic mice older than 9 months were divided into two groups of three mice, one group exposed to external mutagenic factors for the development of skin cancers, and the second group exposed to the same mutagenic factors concomitantly with a daily administration of cabozantinib at 30 mg/kg by gavage. Six wild-type mice of the same age and from the same background served as control, and were exposed to the same mutagenic factors than mutated transgenic mice.

We started tumor induction by a single topical application of 20 μg of 7,12-dimethylbenz[*a*]anthracene (DMBA) (Sigma-Aldrich) in 0.1 mL acetone on the backs of mice. Two days later, we started UVB exposition at 380 mJ/cm^2 twice a week until the development of skin tumors, using Waldmann UV 109 B UV lamp. For the group of mutated mice receiving cabozantinib, the drug administration was initiated 14 days before we started tumor induction. Skin tumors were counted from the moment they appeared, and tumor growth was measured twice weekly in two perpendicular diameters with a caliper. Tumor volumes were calculated as following: $V = L \times l^2\ 2$, L being the larger diameter (length), l the smaller (width). At euthanasia, mice were dissected as describe above.

Results

Index-case: a young woman with cancer and other severe diseases

A 36-year-old woman was diagnosed with concomitant localized breast cancer overexpressing HER2, and polycythemia vera with *JAK2* V617F mutation, together with definite rheumatoid arthritis (9).

A thorough analysis of the patient's family history showed a third-generation papillary thyroid cancer in a paternal aunt (III,9), and four patrilineal breast cancers and one colon cancer in the second generation (Supplementary Fig. S2). However, in our patient, no mutation was found in breast cancer predisposition genes of high penetrance (*BRCA1*, *BRCA2*, *TP53*, *PTEN*) or of moderate penetrance (*CHEK2*, *PALB2* and *ATM*).

Identification of a constitutional *MET* mutation

To look for mutations in other candidate genes of low to moderate penetrance in our patient (index-case), we chose an original approach, and performed genomic analyses for copy number variations and point mutations on laser-microdissected tumor cells from the breast cancer, and on CD34$^+$ cells sorted from bone marrow aspiration. Using ONCOSCAN technology dedicated to formalin-fixed tumor samples (Supplementary Fig. S1), and a threshold of 9 for probability scores to filter the data, we identified 17 mutations (Table 1). Over 541 mutations tested, only pR988C, c2962C_T *MET* mutation was common to the two cell populations, with a probability score of 48.5 and 34.1 for breast cancer and CD34$^+$ cells, respectively (Table 1 in bold).

When we focused on copy number variations, the most common events were LOH in noncoding sequences (Supplementary Table S1). One LOH, located in chromosome 3p25.3 with von Hippel Lindau (*VHL*) and *FANCD2* genes, was common to the breast cancer and CD34$^+$ cells. No common hotspot *VHL* mutation was identified in either breast cancer or CD34$^+$ cells.

Using DNA-HRM and sequencing, we confirmed the presence of pR988C, c2962C>T heterozygous *MET* mutation in laser-microdissected breast cancer cells, CD34$^+$ bone marrow cells, and constitutional DNA from hair bulb (Fig. 1A). Because we had the opportunity to test the thyroid cancer of our patient's paternal aunt (III;9 on Supplementary Fig. S2), we found the same pR988C, c2962C>T *MET* mutation, enabling us to confirm that this was a familial mutation from the paternal side. MET protein was also overexpressed by tumor cells in the thyroid cancer (Fig. 1B).

For the *VHL* locus, using microsatellite markers (Supplementary Fig. S3), breast cancer cells had *VHL* LOH, in accordance

Published OnlineFirst April 19, 2019; DOI: 10.1158/1078-0432.CCR-18-3261

Table 1. List of identified hot-spot mutations in breast cancer cells and in CD34-positive bone marrow cells using ONCOSCAN technology

	Probability score	Gene	Mutation	Chromosome
Breast cancer	**48.5**	***MET***	**pR988C, c2962C_T**	**7**
	9.8	*HRAS*	pG12S, c34G_A	11
CD34-positive bone marrow cells	**34.1**	***MET***	**pR988C, c2962C_T**	**7**
	18.1	*PTEN*	pI101T, c302T_C	10
	13	*NF2*	pQ362X, c1084C_T	22
	12.6	*FGFR3*	pA369A, c1107G_T	4
	12.3	*HRAS*	pG12D, c35G_A	11
	12.1	*SMARCB1*	pR201X, c601C_T	22
	11.9	*RB1*	pR455X, c1363C_T	13
	11.8	*RB1*	pR787X, c2359C_T	13
	11.3	*VHL*	pE160K, c478G_A	3
	10.4	*NF2*	pR196X, c586C_T	22
	10.2	*RB1*	pQ702X, c2104C_T	13
	10	*CTNNB1*	pS45P, c133T_C	3
	9.5	*APC*	pR1450X, c4348C_T	5
	9.5	*NF2*	pQ456X, c1366C_T	22
	9.4	*MEN1*	p_c654_plus_3A_G	11
	9	*ABL1*	pF359V, c1075T_G	9

with ONCOSCAN results. $CD34^+$ bone marrow cells and constitutional DNA from our patient had a profile of allelic imbalance, suggesting mosaicism for *VHL* LOH. In contrast, the microsatellite profile of the aunt's thyroid cancer (III;9) was normal, confirming that *VHL* abnormalities occurred *de novo* in our patient.

Identification of the same pR988C, c2962C>T *MET* mutation in two series of patients with sporadic breast cancer or polycythemia vera with *JAK2* V617F mutation

In a series of 105 sporadic breast cancers from Saint-Louis Hospital (Paris, France), we used DNA-HRM to detect pR988C, c2962C>T *MET* mutation. It was identified in one patient with a triple negative ductal carcinoma of the breast.

We also tested total blood DNA from 96 patients with *JAK2* V617F-mutated polycythemia vera. Using DNA-HRM, the pR988C, c2962C>T *MET* mutation was identified in one 87-year-old patient. Surprisingly, she also had personal history of rheumatoid arthritis and cryoglobulinemia.

An innovative approach to establish transgenic mice for pR988C, c2962C>T *MET* mutation

Because the pR988C, c2962C>T *MET* mutation is located on a codon identical in human and mouse genes, we decided to establish knock-in transgenic mice to decipher the function of this point mutation.

Using CRISPR-Cas9 technology, one cell stage embryos from C57Bl6 females were microinjected with ssDNA oligonucleotides as mutation donor, two types of sgRNA and two concentrations of Cas9 enzyme and sgRNA, either into the cytoplasm or into the nucleus. After incubation and cell division up to the blastocyst stage (around 100 cells), the blastocysts were tested for the integration of the pR988C, c2962C>T *MET* mutation. Using the enzymatic restriction method and DNA-HRM, we were able to ascertain whether our method was successful before embryo reimplantation. We could thus determine the optimal condition, with a ratio of 50 ng/20 ng of Cas9/sgRNA microinjected directly into the nucleus resulting in 19% to 25% of the embryos harboring the mutation (Supplementary Table S2).

Twenty-one days after reimplantation, a first generation of 17 mice was obtained, including 4 mutated animals (23.5%), 2 of them with both pR988C *MET* mutation and an indel (mice 8, 10, 12, and 19, see Supplementary Fig. S4). Second and third generations, obtained through heterozygous mating and mainly successful for Founders 10 and 12, led to the elimination of indel, and of potential off-targets for 2 mice (Supplementary Figs. S4 and S5B). A total of 23 mutated mice were thus obtained, characterized by genotyping using enzymatic restriction, DNA-HRM and sequencing. Copy number variation was performed for all mice with a ratio mutated *MET*/*TFrc* reference gene ranging from 0.5 to 12 (Supplementary Fig. S5). Unfortunately, we were not able to obtain successful mating after the third generation, either through heterozygous or homozygous coupling.

Transgenic mice for the pR988C, c2962C>T *MET* mutation developed autoimmune diseases and cancer

From the age of 9 months, all mutated mice had histologic signs of Sjögren syndrome, characterized by a dense periductal lymphocyte infiltrate (Chisholm score of III or IV) in the salivary and lachrymal glands. To confirm a potential autoimmune disease associated with the *MET* mutation, we used ELISA to monitor serum levels of anti-SSA and anti-SSB murine antibodies. Both were significantly higher in mutated mice than in wild-type mice ($P < 0.05$). In 11 of 12 mutated mice, we also found histologic signs of synovial hyperplasia and an inflammatory infiltrate in the distal but not proximal joints. Serum levels of anticyclic citrullinated peptide (anti-CPP also called ACPA) and of anti-dsDNA antibodies were significantly higher in the mutated mice than in the wild-type mice ($P < 0.01$; Fig. 2).

We found signs of thyroiditis in 8 of 12 mice. One 10-month-old mutated mouse (II:10) also developed a skin squamous cell carcinoma on the ear. Wild-type mice had no sign of Sjögren syndrome, arthritis or cancer.

Transgenic mice for pR988C, c2962C>T *MET* mutation developed myeloproliferative syndromes

Blood cell counts, obtained at 1, 6, and 9 months for 12 mutated mice, showed a significant increase in platelet numbers in the mutated mice compared with the wild-type mice from 1 month on (mean numbers at 9 months of $1{,}078.10^3/mm^3$ (± 137) and $775.10^3/mm^3$ (± 282), respectively, $P < 0.05$ (Fig. 3A). There was a trend for an increase in red blood cell numbers (mean numbers at 9 months of $10.7 \times 10^6/mm^3$ and $9.4 \times 10^6/mm^3$ respectively, $P = 0.07$; Fig. 3A).

Published OnlineFirst April 19, 2019; DOI: 10.1158/1078-0432.CCR-18-3261

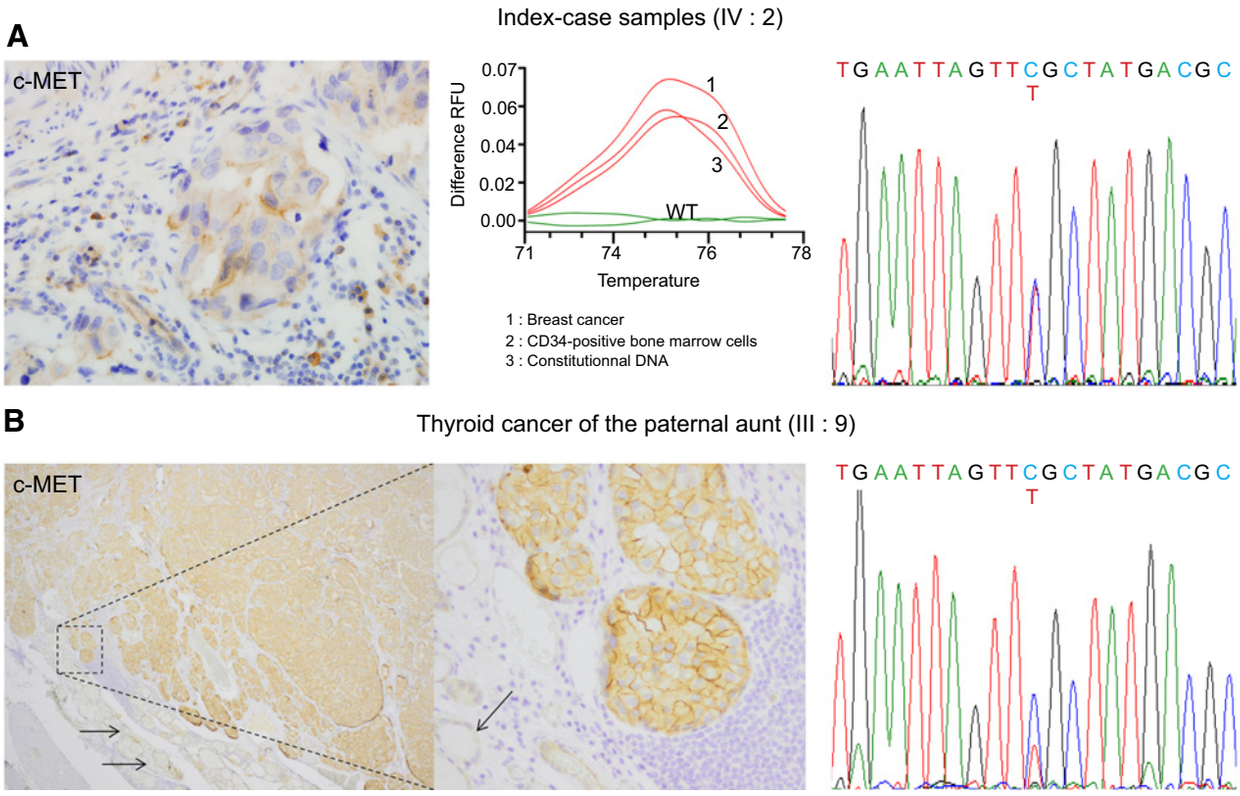

Figure 1.

A, c-MET (clone SP 44) expression in breast cancer cells. PCR-HRM for pR988C *MET* mutation in laser-microdissection breast cancer cells, CD34-positive bone marrow cells, and constitutional DNA from the index case shows a profile different from wild-type profile. Sequencing of the three samples confirms the presence of a heterozygous pR988C,c2962C>T *MET* mutation. **B,** c-MET (clone SP 44) expression in thyroid carcinoma. All tumor cells show high membranous expression (left, ×20 and right, ×200). Normal thyroid follicles are negative (arrows). Sequencing of DNA from this thyroid carcinoma also evidences the heterozygous pR988C,c2962C>T *MET* mutation.

Flow cytometry analyses of bone marrow were obtained for 8 mutated mice and 8 wild-type mice to assess percentages of different lineages (Fig. 3B and C). For LK populations, we found that the mutated mice had higher bone marrow cell densities than wild-type mice, with absolute cell counts of 24.1×10^6 (± 2.6) versus 9.4×10^6 (± 1.1), respectively ($P < 0.01$, Fig. 3D). These higher cell densities were found in all three myeloid progenitor lineages (Fig. 3E). The largest numbers were found for the granulocyte macrophage progenitors, GMP (Fig. 3F).

Tissue section analyses confirmed the higher bone marrow density in mutated mice than in wild-type mice. In addition, voluminous ovaries were found in two mutated mice. Microscope examination showed extramedullary hematopoietic proliferation with bone differentiation in these two voluminous ovaries (Fig. 3G).

Functional inhibition of the MET pathway

Activation of the MET/HGFR transmembrane receptor induces MET dimerization, phosphorylation of tyrosines Y1234 and Y1235 in the tyrosine kinase (TK) domain, and of Y1349 and Y1356 in the carboxyl terminal region, leading to downstream signals (Supplementary Fig. S6; ref. 10). The highly conserved juxta-membrane domain (JM) acts as a negative regulator of signal transduction, enabling MET ubiquitination and degradation (11). Mutations in the JM domain could suppress this negative regulation (12), and thus lead to constitutive activation of MET.

The pR988C, c2962C>T *MET* mutation is located in the JM domain (Supplementary Fig. S6). Using immunohistochemistry on frozen liver samples and an anti-phosphoMET recognizing the phosphorylated tyrosine 1349 in the murine carboxyl terminal domain of MET receptor, we showed a higher pMET expression on mutated compared to wild-type liver samples (Fig. 4A). To decipher the functional value of pR988C, c2962C>T *MET* mutation, we administered a MET inhibitor of the TK domain, cabozantinib, to 4 mutated mice for 28 days. On successive bone marrow aspiration samples and blood analyses (day 0, day 28, and day 42), this MET pathway inhibition led to a decrease of GMP in the bone-marrow of the mutated mice and a drop in red blood cell counts and hemoglobin level, and to a normalization of serum concentration of anti-CCP and anti-SSB antibodies at day 28 in the mutated mice. These effects were followed by redundancy after the 14-day wash-out period (Fig. 4).

To sum up, CRISPR-Cas9 technology enabled us to establish pR988C *MET*-mutated transgenic mice that reproduced the autoimmune diseases and myeloproliferation found in our index-case. The use of an anti-MET drug validated the functional role of this mutation, and of the MET pathway activation in the maintenance of myeloproliferation, rheumatoid arthritis, and Sjögren syndrome.

Published OnlineFirst April 19, 2019; DOI: 10.1158/1078-0432.CCR-18-3261

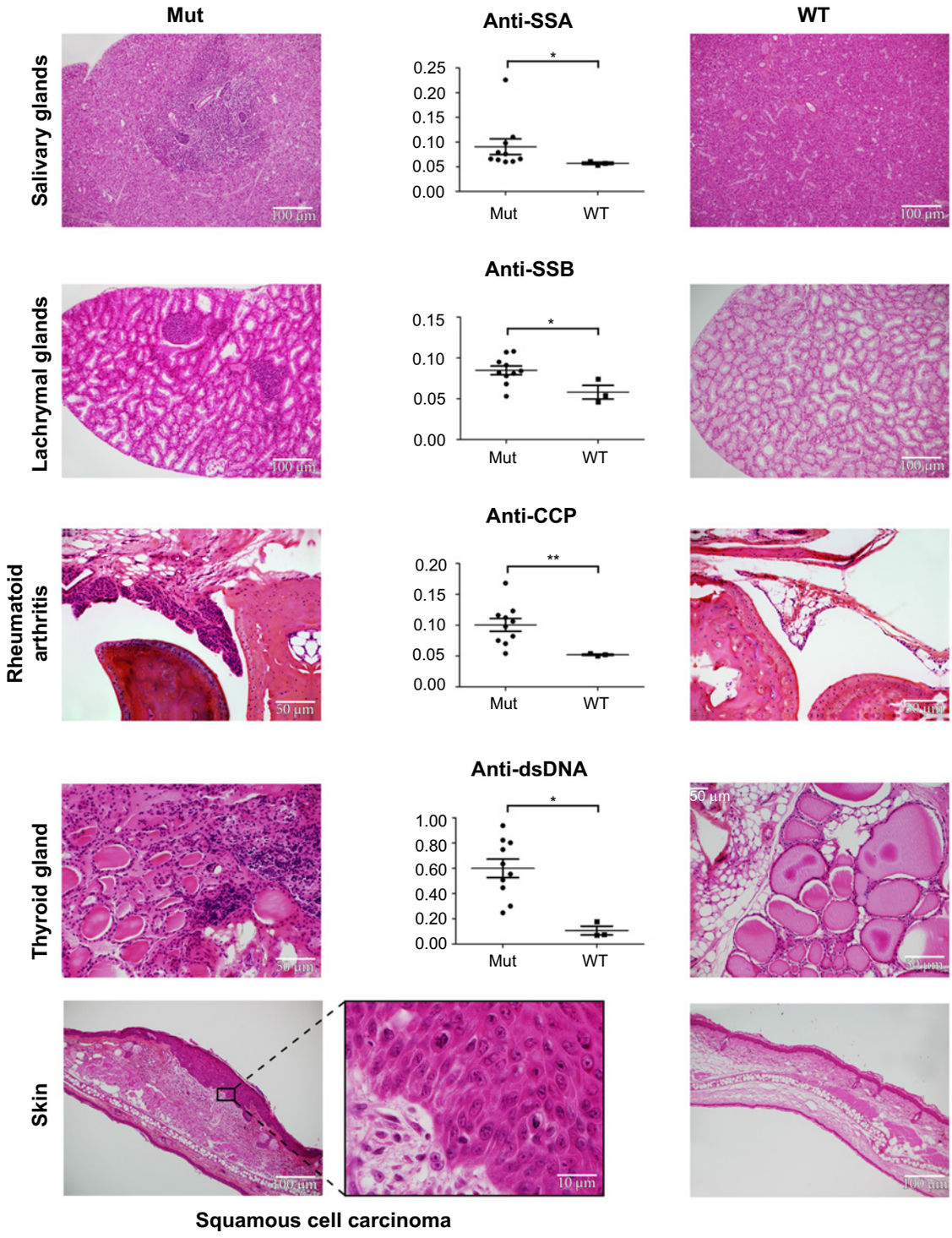

Figure 2.

Transgenic mice for the pR988C,c2962C>T *MET* mutation develop autoimmune diseases and cancer. Figure 2 illustrates the phenotypes of one pR988C *MET*-mutated transgenic mouse (left) and one wild-type mouse (right). It shows a typical Sjögren syndrome in salivary and lachrymal glands of the transgenic mouse with dense periductal lymphocyte infiltrates. Using ELISA, serum levels of anti-SSA and anti-SSB murine antibodies are significantly higher in the mutated mouse than in the wild-type mouse. Figure 2 also shows histologic signs of synovial hyperplasia of a distal joint in the mutated mouse concomitant with high serum levels of anti-CCP antibody, and signs of thyroiditis with lymphocyte infiltrate between abnormal thyroid follicles. Bottom left, skin squamous cell carcinoma of the ear at low magnification (×2.5). At higher magnification (×40), malignant epithelial cells are invading the derm.

Published OnlineFirst April 19, 2019; DOI: 10.1158/1078-0432.CCR-18-3261

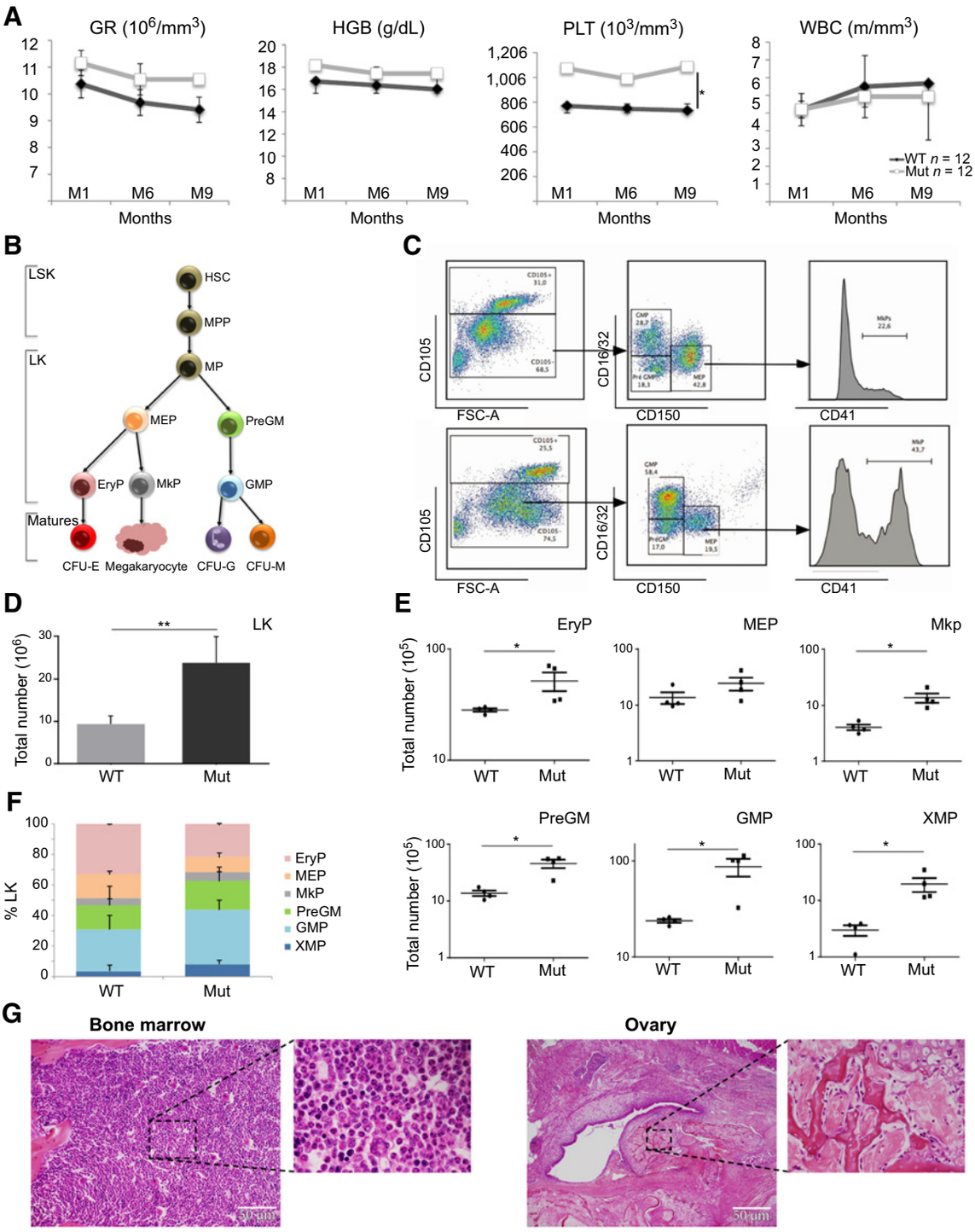

Figure 3.

Transgenic mice for the pR988C,c2962C>T *MET* mutation develop myeloproliferative syndromes. **A,** Blood cell counts at 1, 6, and 9 months show a significant increase in platelet numbers in the mutated mice compared with the wild-type mice from 1 month on. *, $P < 0.05$. **B,** Illustration of the different myeloid lineages. **C,** Flow cytometry analysis of bone marrow from a mutated mouse (bottom) shows a different profile from a wild-type mouse (top). **D,** The mutated mice ($n = 8$) have significantly higher bone marrow cell densities that wild-type mice ($n = 8$). **, $P < 0.01$. **E,** The higher cell densities are found in all three myeloid progenitor lineages, in particular in EryP, MkP, preGMP, and GMP populations. *, $P < 0.05$. **F,** The largest numbers are found for GMP population that represents 39% of total LK population in mutated mice compared with 28% in wild-type mice. **G,** Tissue section of a sternum confirms the high bone marrow density (left). Histologic analysis of a voluminous macroscopic ovary (right) shows extramedullary hematopoietic proliferation with bone differentiation.

Published OnlineFirst April 19, 2019; DOI: 10.1158/1078-0432.CCR-18-3261

Additional mutagenic factors are required for cancerogenesis

We hypothesized that pR988C *MET* mutation is of moderate penetrance for cancerogenesis and thus requires additional mutational factors to induce cancers. Because one of the transgenic mice spontaneously developed a skin squamous cell carcinoma of the ear, we decided to expose 3 transgenic mice and 6 control wild-type mice to two additional mutagenic factors, including one chemical factor DMBA, and Ultraviolet B radiation UVB (Fig. 5A). After 2 months, the mean number of skin cancers per mouse was significantly higher in the *MET*-mutated mice compared with

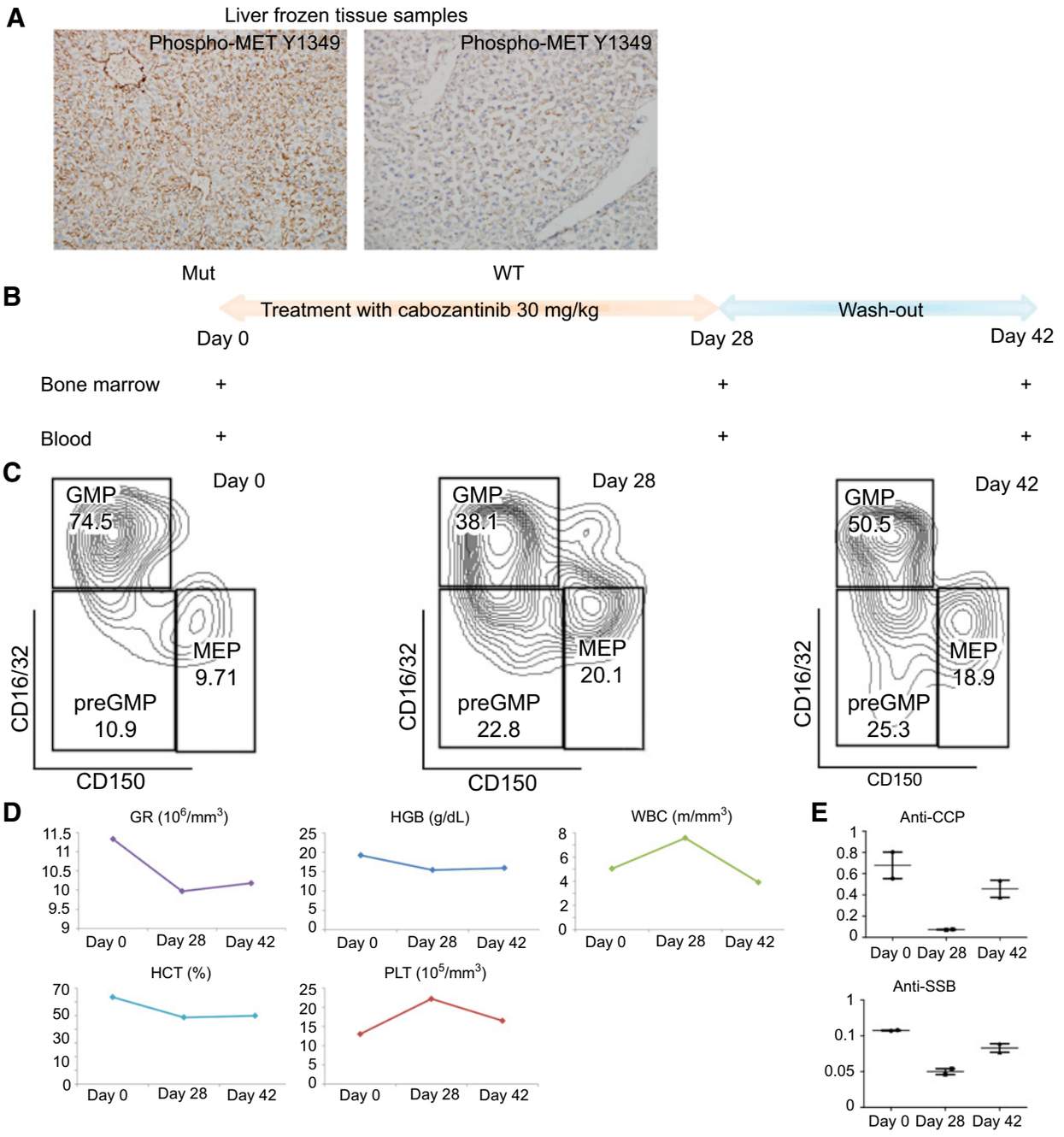

Figure 4.

Functional inhibition of the MET pathway. **A,** On frozen liver samples, using IHC phospho-MET Y1349 is more expressed on mutated (Mut) compared with wild-type (WT) samples. **B,** Treatment plan of mutated mice with 28 days of continuous treatment with cabozantinib, a MET inhibitor, at the daily dose of 30 mg/kg followed by a 14-day wash-out period. **C,** Flow cytometry on successive bone marrow aspiration samples shows a decrease of GMP population at day 28 compared with day 0, followed by a redundancy at day 42 after the wash-out period. **D** and **E,** Successive blood analyses performed at the same time points show a drop in red blood cell counts and hemoglobin level (**D**), and a normalization of serum concentrations of anti-SSB and anti-CCP antibodies at day 28 (**E**). These effects are also followed by a redundancy after the wash-out period.

Published OnlineFirst April 19, 2019; DOI: 10.1158/1078-0432.CCR-18-3261

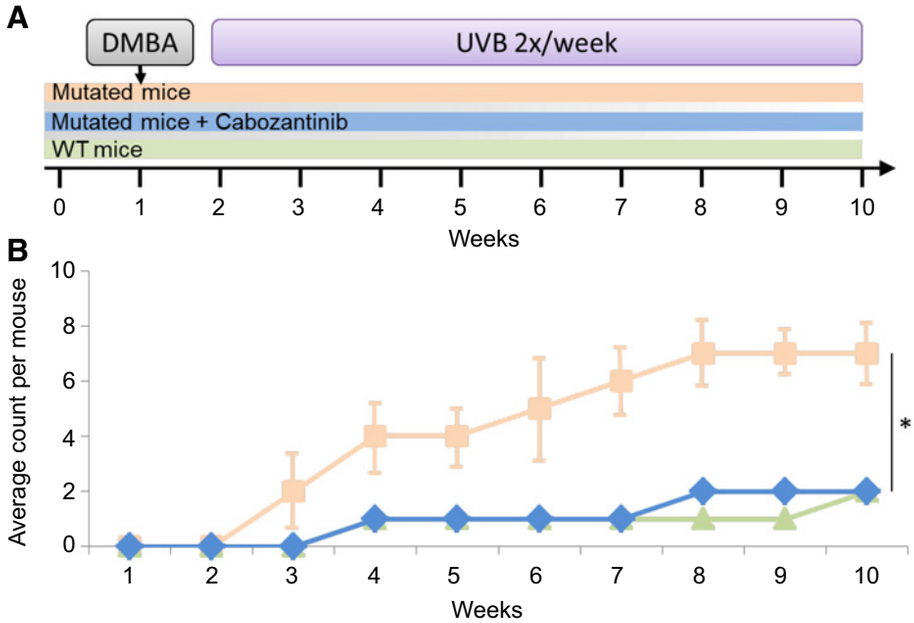

Figure 5.
Additional mutagenic factors are required for carcinogenesis. **A,** Schedule of exposure to mutagenic factors for the three different arms: *MET*-mutated mice, *MET*-mutated mice concomitantly treated with cabozantinib, and wild-type mice. **B,** Mean number of skin cancers is significantly higher in *MET*-mutated mice compared with wild-type mice and to *MET*-mutated mice treated with cabozantinib. *, $P < 0.05$. DMBA: 7,12-dimethylbenz [*a*]anthracene; UVB: ultraviolet B.

wild-type mice (7 vs. 1.8, $P < 0.05$). One of the *MET*-mutated mice also developed a thyroid carcinoma.

To confirm the role of pR988C *MET* mutation in activating MET pathway for cancerogenesis, we gave cabozantinib to 3 *MET*-mutated mice before exposing them to DMBA and UVB.

The regimen with cabozantinib significantly reduced the number of skin cancers when compared with *MET* mutated mice ($P < 0.05$, Fig. 5B).

Discussion

Here, we demonstrated the feasibility of an individual approach in constitutional genetics: (i) by studying several samples from different lesions in a same young patient, (ii) by using high-speed technologies dedicated to whole-genome analysis, (iii) by using CRISPR-Cas9 technology to establish knock-in transgenic mice for a variant of interest, within few months. We were thus able to demonstrate the functional value of the pR988C, c2962C>T *MET* mutation, and its involvement in the genesis of myeloproliferative neoplasms and autoimmune diseases, an important link not previously identified.

Sjögren syndrome and rheumatoid arthritis are frequently associated (13), and familial aggregations have been reported (14). Genome-wide association studies have identified more than 10 susceptibility alleles of unknown functional value, such as *HLA-DRB1*, *IRF5*, *STAT4*, or *BLK* (15–19). Here, we demonstrated the role of constitutional genetics in the initiation and development of Sjögren syndrome and rheumatoid arthritis, with high phenotypic penetrance of pR988C, c2962C>T *MET* mutation in our murine model. On the basis of these experimental results, we inquired about the occurrence of these two autoimmune diseases in the family of our index-case, and found that her father (III,8) and her paternal grand-father (II,3) had rheumatoid arthritis (Supplementary Fig. S11).

To confirm the role of the MET pathway in the development of Sjögren syndrome and rheumatoid arthritis, we used the drug cabozantinib to inhibit the MET pathway in our mouse model. After 4 weeks of drug exposure, serum concentrations of specific auto-antibodies, anti-SSB and anti-CCP, were normalized. Previously, the role of HGF, the only ligand of MET (20), has been proposed in rheumatoid arthritis. In 136 patients, high HGF plasma levels were associated with severe joint destruction (21), and experimental HGF blockade using NK4, a HGF inhibitor, decreased arthritis lesions in mice (22). Here, we demonstrated the role of MET receptor activation in Sjögren syndrome and rheumatoid arthritis.

As a whole, these clinical and experimental results open the way for a new targeted therapy consisting in testing MET inhibitors, already available in clinical practice, among patients with rheumatoid arthritis, Sjögren syndrome, and MET pathway activation. A preliminary step is to assess the incidence of constitutional pR988C, c2962C>T MET mutation in cohorts of patients with rheumatoid arthritis or Sjögren syndrome, using cohorts like the French "ESPOIR" cohort, which includes patients with early arthritis followed up over a number of years (23, 24).

Patients with autoimmune diseases have a 20% increased risk of developing myeloproliferative neoplasms (25), including polycythemia vera as in our index-case. The chronic inflammation of autoimmune diseases could generate mutations in hematopoietic stem cells (26), particularly for *JAK2* V617F mutation (27), what found in our index-case (see Table 1). In 96 other patients with *JAK2*-mutated polycythemia vera, we identified the pR988C *MET* mutation in blood DNA in one case, and this woman also had cryoglobulinemia and rheumatoid arthritis. The genetic origin of myeloproliferative neoplasms is established for somatic mutations in *JAK2*, *CALR* or *MPL*, which drive clonal proliferation, but only candidate polymorphisms have been identified through genome-wide association studies for constitutional genetics (28). Here, we demonstrated that the pR988C, c2962C>T *MET* mutation was sufficient to generate a myeloproliferation in all mutated mice. In addition, the involvement of the three myeloid lineages is an argument for a functional effect of this mutation at an early stage of myeloid progenitor commitment. As in Sjögren syndrome or rheumatoid arthritis (21, 29), the HGF

Published OnlineFirst April 19, 2019; DOI: 10.1158/1078-0432.CCR-18-3261

level is increased in the serum of patients with polycythemia vera, independently from the *JAK2* V617F mutation (30).

Our index-case developed rheumatoid arthritis and polycythemia vera in a context of constitutional pR988C, c2962C>T *MET* mutation. We were able to reproduce this phenotype in mice transgenic for the *MET* mutation. But our index-case had also developed breast cancer, and her paternal aunt had thyroid cancer with pR988C *MET* mutation.

MET is a proto-oncogene (31), and nonsense activating mutations have been found in the TK domain of patients with hereditary papillary kidney cancers (32–34). Somatic mutations have mainly been identified in the TK- and SEMA-domains of *MET* in childhood hepatocellular carcinomas, and in head and neck, gastric, and lung cancers (Supplementary Fig. S9; ref. 20). The pR988C, c2962C>T *MET* mutation is not located in the TK- or SEMA-domain but in the JM domain (35, 36). This mutation has been reported in thyroid and lung cancers, and to date is considered as sporadic (37, 38). Here, the analysis of several lesions from the same patient, combined with family investigation, led us to demonstrate that, in this case, the pR988C mutation of *MET* was constitutional. When we tested a series of 105 breast cancers without history of familial breast cancer, we found this *MET* mutation in one other case; unfortunately, we were not able to perform any familial investigation, as the patient had died. These familial investigations, mainly based on retrospective data analyses, can be difficult to perform. However, our study does raise the question of whether constitutional mutations contribute to cancers so far considered as sporadic.

We did not reproduce spontaneous breast or thyroid cancers, but the systematic pathologic study found lymphocytic thyroiditis in 14 of 23 transgenic mice when, in patients, chronic lymphocytic thyroiditis is associated with a 2-fold increased risk of papillary thyroid cancer (39). In addition, one of the transgenic mice developed a skin squamous cell carcinoma of the ear, as observed in mice transgenic for HGF with a strong activation of the MET pathway (40). We reproduced experimentally the occurrence of skin carcinomas in our transgenic mice, and reduced significantly the number of cancers by concomitant administration of a MET inhibitor demonstrating that MET activation is sufficient for increasing the susceptibility to skin cancer. The activation of the MET pathway may be too low for spontaneous carcinogenesis in our transgenic mice with pR988C MET mutation, and likewise in our patient. Additional molecular abnormalities are probably required, including mutations in other oncogenes or tumor suppressor genes. Mutations in the JM domain suppress MET receptor ubiquitination and degradation in human lung cancer cell lines (12, 20), but the level of MET pathway activation is not known. In another transgenic model for MET-activating mutation in the TK domain, considerable amplification of the MET gene was required for the development of breast cancer (20, 41). High serum levels of HGF were found with breast cancer development in mice transgenic for HGF (42). Autocrine/paracrine loops could also explain this increased activation of the MET pathway in cancer cells compared to normal cells, as described in multiple myeloma (43, 44).

In our index-case, we found a constitutional LOH including *FANCD2* in addition to the pR988C *MET* mutation. *FANCD2* is a gene implicated in DNA repair (45), as are *BRCA* genes, responsible for hereditary breast cancers. This reinforces the role of constitutional genetics in the development of cancers usually considered as sporadic.

Our approach combining the study of cell and tissue samples of several lesions in the same patient, the use of high-throughput genomic analyses, and of CRISPR-Cas9 technology enabled us to demonstrate for the first time a functional genetic link between Sjögren syndrome, rheumatoid arthritis, polycythemia vera, and cancers. It opens a field of application for this individual approach in the domain of constitutional genetics.

Disclosure of Potential Conflicts of Interest

J. Kiladjian reports receiving commercial research grants from Novartis and is a consultant/advisory board member for Novartis, Celgene, and AOP Orphan. No potential conflicts of interest were disclosed by the other authors.

Authors' Contributions

Conception and design: M. El Bouchtaoui, I. Loisel-Ferreira, C. Ferreira, A. Janin, G. Bousquet
Development of methodology: M. El Bouchtaoui, I. Loisel-Ferreira, C. Fedronie, G. Falgarone, G. Bousquet
Acquisition of data (provided animals, acquired and managed patients, provided facilities, etc.): M. El Bouchtaoui, M. Do Cruzeiro, C. Leboeuf, R. Ait El Far, M. Ziol, M. Espié, G. Falgarone, B. Cassinat, J.-J. Kiladjian, A. Janin, G. Bousquet
Analysis and interpretation of data (e.g., statistical analysis, biostatistics, computational analysis): M. El Bouchtaoui, C. Leboeuf, G. Falgarone, J.-J. Kiladjian, J.-P. Feugeas, A. Janin, G. Bousquet
Writing, review, and/or revision of the manuscript: M. El Bouchtaoui, M. Do Cruzeiro, C. Leboeuf, I. Loisel-Ferreira, C. Ferreira, M. Espié, G. Falgarone, B. Cassinat, J.-J. Kiladjian, A. Janin, G. Bousquet
Administrative, technical, or material support (i.e., reporting or organizing data, constructing databases): C. Leboeuf, G. Falgarone, G. Bousquet
Study supervision: A. Janin, G. Bousquet
Other (establishment of mouse model MET by CRISPR approach and maintenance of the line): M. Do Cruzeiro

Acknowledgments

We would like to thank Mrs A. Swaine for revising the English language. We also would like to thank Prof. Jessica Zucman-Rossi, Prof. Hugues de Thé, and Dr. Marie Dutreix for their helpful critical review of the manuscript. This work was supported by Inserm, University Paris 7.

The costs of publication of this article were defrayed in part by the payment of page charges. This article must therefore be hereby marked *advertisement* in accordance with 18 U.S.C. Section 1734 solely to indicate this fact.

Received October 10, 2018; revised February 16, 2019; accepted April 15, 2019; published first April 19, 2019.

References

1. Pearlman R, Frankel WL, Swanson B, Zhao W, Yilmaz A, Miller K, et al. Prevalence and spectrum of germline cancer susceptibility gene mutations among patients with early-onset colorectal cancer. JAMA Oncol 2017;3:464–71.
2. Shiovitz S, Korde LA. Genetics of breast cancer: a topic in evolution. Ann Oncol 2015;26:1291–9.
3. Wooster R, Neuhausen SL, Mangion J, Quirk Y, Ford D, Collins N, et al. Localization of a breast cancer susceptibility gene, BRCA2, to chromosome 13q12-13. Science 1994;265:2088–90.
4. Hsieh YC, Tu SH, Su CT, Cho EC, Wu CH, Hsieh MC, et al. A polygenic risk score for breast cancer risk in a Taiwanese population. Breast Cancer Res Treat 2017;163:131–8.

5. Long J, Cai Q, Sung H, Shi J, Zhang B, Choi JY, et al. Genome-wide association study in east Asians identifies novel susceptibility loci for breast cancer. PLoS Genet 2012;8:e1002532.
6. Zhang B, Beeghly-Fadiel A, Long J, Zheng W. Genetic variants associated with breast-cancer risk: comprehensive research synopsis, meta-analysis, and epidemiological evidence. Lancet Oncol 2011;12:477–88.
7. Pena-Llopis S, Vega-Rubin-de-Celis S, Liao A, Leng N, Pavia-Jimenez A, Wang S, et al. BAP1 loss defines a new class of renal cell carcinoma. Nat Genet 2012;44:751–9.
8. Farley MN, Schmidt LS, Mester JL, Pena-Llopis S, Pavia-Jimenez A, Christie A, et al. A novel germline mutation in BAP1 predisposes to familial clear-cell renal cell carcinoma. Mol Cancer Res 2013;11:1061–71.
9. Aletaha D, Neogi T, Silman AJ, Funovits J, Felson DT, Bingham CO III, et al. 2010 Rheumatoid arthritis classification criteria: an American College of Rheumatology/European League Against Rheumatism collaborative initiative. Arthritis Rheum 2010;62:2569–81.
10. Matsumoto K, Umitsu M, De Silva DM, Roy A, Bottaro DP. Hepatocyte growth factor/MET in cancer progression and biomarker discovery. Cancer Sci 2017;108:296–307.
11. Peschard P, Fournier TM, Lamorte L, Naujokas MA, Band H, Langdon WY, et al. Mutation of the c-Cbl TKB domain binding site on the Met receptor tyrosine kinase converts it into a transforming protein. Mol Cell 2001;8: 995–1004.
12. Kong-Beltran M, Seshagiri S, Zha J, Zhu W, Bhawe K, Mendoza N, et al. Somatic mutations lead to an oncogenic deletion of met in lung cancer. Cancer Res 2006;66:283–9.
13. Fallahi P, Ferrari SM, Ruffilli I, Elia G, Biricotti M, Vita R, et al. The association of other autoimmune diseases in patients with autoimmune thyroiditis: review of the literature and report of a large series of patients. Autoimmun Rev 2016;15:1125–8.
14. Sabio JM, Milla E, Jimenez-Alonso J. A multicase family with primary Sjogren's syndrome. J Rheumatol 2001;28:1932–4.
15. Lessard CJ, Li H, Adrianto I, Ice JA, Rasmussen A, Grundahl KM, et al. Variants at multiple loci implicated in both innate and adaptive immune responses are associated with Sjogren's syndrome. Nat Genet 2013;45: 1284–92.
16. Li Y, Zhang K, Chen H, Sun F, Xu J, Wu Z, et al. A genome-wide association study in Han Chinese identifies a susceptibility locus for primary Sjogren's syndrome at 7q11.23. Nat Genet 2013;45:1361–5.
17. Gregersen PK, Silver J, Winchester RJ. The shared epitope hypothesis. An approach to understanding the molecular genetics of susceptibility to rheumatoid arthritis. Arthritis Rheum 1987;30:1205–13.
18. Gourraud PA, Dieude P, Boyer JF, Nogueira L, Cambon-Thomsen A, Mazieres B, et al. A new classification of HLA-DRB1 alleles differentiates predisposing and protective alleles for autoantibody production in rheumatoid arthritis. Arthritis Res Ther 2007;9:R27.
19. Korman BD, Kastner DL, Gregersen PK, Remmers EF. STAT4: genetics, mechanisms, and implications for autoimmunity. Curr Allergy Asthma Rep 2008;8:398–403.
20. Graveel CR, Tolbert D, Vande Woude GF. MET: a critical player in tumorigenesis and therapeutic target. Cold Spring Harb Perspect Biol 2013;5:pii: a009209.
21. Grandaunet B, Syversen SW, Hoff M, Sundan A, Haugeberg G, van Der Heijde D, et al. Association between high plasma levels of hepatocyte growth factor and progression of radiographic damage in the joints of patients with rheumatoid arthritis. Arthritis Rheum 2011;63:662–9.
22. Tsunemi S, Iwasaki T, Kitano S, Matsumoto K, Takagi-Kimura M, Kubo S, et al. Molecular targeting of hepatocyte growth factor by an antagonist, NK4, in the treatment of rheumatoid arthritis. Arthritis Res Ther 2013;15:R75.
23. Combe B, Benessiano J, Berenbaum F, Cantagrel A, Daures JP, Dougados M, et al. The ESPOIR cohort: a ten-year follow-up of early arthritis in France: methodology and baseline characteristics of the 813 included patients. Joint Bone Spine 2007;74:440–5.
24. Salliot C, Dawidowicz K, Lukas C, Guedj M, Paccard C, Benessiano J, et al. PTPN22 R620W genotype-phenotype correlation analysis and gene-environment interaction study in early rheumatoid arthritis: results from the ESPOIR cohort. Rheumatology 2011;50:1802–8.
25. Kristinsson SY, Landgren O, Samuelsson J, Bjorkholm M, Goldin LR. Autoimmunity and the risk of myeloproliferative neoplasms. Haematologica 2010;95:1216–20.
26. Sorensen AL, Hasselbalch HC. Antecedent cardiovascular disease and autoimmunity in Philadelphia-negative chronic myeloproliferative neoplasms. Leuk Res 2016;41:27–35.
27. Barbui T, Carobbio A, Finazzi G, Vannucchi AM, Barosi G, Antonioli E, et al. Inflammation and thrombosis in essential thrombocythemia and polycythemia vera: different role of C-reactive protein and pentraxin 3. Haematologica 2011;96:315–8.
28. Tapper W, Jones AV, Kralovics R, Harutyunyan AS, Zoi K, Leung W, et al. Genetic variation at MECOM, TERT, JAK2 and HBS1L-MYB predisposes to myeloproliferative neoplasms. Nat Commun 2015;6:6691.
29. Balarini GM, Zandonade E, Tanure L, Ferreira GA, Sardenberg WM, Serrano EV, et al. Serum calprotectin is a biomarker of carotid atherosclerosis in patients with primary Sjogren's syndrome. Clin Exp Rheumatol 2016;34: 1006–12.
30. Boissinot M, Cleyrat C, Vilaine M, Jacques Y, Corre I, Hermouet S. Anti-inflammatory cytokines hepatocyte growth factor and interleukin-11 are over-expressed in Polycythemia vera and contribute to the growth of clonal erythroblasts independently of JAK2V617F. Oncogene 2011;30: 990–1001.
31. Cooper CS, Park M, Blair DG, Tainsky MA, Huebner K, Croce CM, et al. Molecular cloning of a new transforming gene from a chemically transformed human cell line. Nature 1984;311:29–33.
32. Schmidt L, Duh FM, Chen F, Kishida T, Glenn G, Choyke P, et al. Germline and somatic mutations in the tyrosine kinase domain of the MET proto-oncogene in papillary renal carcinomas. Nat Genet 1997;16:68–73.
33. Schmidt L, Junker K, Weirich G, Glenn G, Choyke P, Lubensky I, et al. Two North American families with hereditary papillary renal carcinoma and identical novel mutations in the MET proto-oncogene. Cancer Res 1998; 58:1719–22.
34. Verine J, Pluvinage A, Bousquet G, Lehmann-Che J, de Bazelaire C, Soufir N, et al. Hereditary renal cancer syndromes: an update of a systematic review. Eur Urol 2010;58:701–10.
35. The Cancer Genome Atlas Research Network. Comprehensive molecular profiling of lung adenocarcinoma. Nature 2014;511:543–50.
36. Reungwetwattana T, Ou SH. MET exon 14 deletion (METex14): finally, a frequent-enough actionable oncogenic driver mutation in non-small cell lung cancer to lead MET inhibitors out of "40 years of wilderness" and into a clear path of regulatory approval. Transl Lung Cancer Res 2015;4:820–4.
37. Tyner JW, Fletcher LB, Wang EQ, Yang WF, Rutenberg-Schoenberg ML, Beadling C, et al. MET receptor sequence variants R970C and T992I lack transforming capacity. Cancer Res 2010;70:6233–7.
38. Boland JM, Jang JS, Li J, Lee AM, Wampfler JA, Erickson-Johnson MR, et al. MET and EGFR mutations identified in ALK-rearranged pulmonary adenocarcinoma: molecular analysis of 25 ALK-positive cases. J Thorac Oncol 2013;8:574–81.
39. Lai X, Xia Y, Zhang B, Li J, Jiang Y. A meta-analysis of Hashimoto's thyroiditis and papillary thyroid carcinoma risk. Oncotarget 2017;8: 62414–24.
40. Cataisson C, Michalowski AM, Shibuya K, Ryscavage A, Klosterman M, Wright L, et al. MET signaling in keratinocytes activates EGFR and initiates squamous carcinogenesis. Sci Signal 2016;9:ra62.
41. Graveel CR, DeGroot JD, Su Y, Koeman J, Dykema K, Leung S, et al. Met induces diverse mammary carcinomas in mice and is associated with human basal breast cancer. Proc Natl Acad Sci U S A 2009;106:12909–14.
42. Ma J, DeFrances MC, Zou C, Johnson C, Ferrell R, Zarnegar R. Somatic mutation and functional polymorphism of a novel regulatory element in the HGF gene promoter causes its aberrant expression in human breast cancer. J Clin Invest 2009;119:478–91.
43. Borset M, Lien E, Espevik T, Helseth E, Waage A, Sundan A. Concomitant expression of hepatocyte growth factor/scatter factor and the receptor c-MET in human myeloma cell lines. J Biol Chem 1996;271: 24655–61.
44. Ferrucci A, Moschetta M, Frassanito MA, Berardi S, Catacchio I, Ria R, et al. A HGF/cMET autocrine loop is operative in multiple myeloma bone marrow endothelial cells and may represent a novel therapeutic target. Clin Cancer Res 2014;20:5796–807.
45. Krzystolik K, Jakubowska A, Gronwald J, Krawczynski MR, Drobek-Slowik M, Sagan L, et al. Large deletion causing von Hippel-Lindau disease and hereditary breast cancer syndrome. Hered Cancer Clin Pract 2014;12:16.

Published OnlineFirst April 19, 2019; DOI: 10.1158/1078-0432.CCR-18-3261

AACR American Association for Cancer Research

Clinical Cancer Research

A Constitutional Activating *MET* Mutation Makes the Genetic Link between Malignancies and Chronic Inflammatory Diseases

Morad El Bouchtaoui, Marcio Do Cruzeiro, Christophe Leboeuf, et al.

Clin Cancer Res 2019;25:4504-4515. Published OnlineFirst April 19, 2019.